Journal of Manufacturing Systems 31 (2012) 162–176

Journal of Manufacturing Systems

journal homepage: www.elsevier.com/locate/jmansys

Technical paper

Variation propagation control in mechanical assembly of cylindrical components

Z. Yang[a,*], A.A. Popov[a], S. McWilliam[b]

[a] Manufacturing Research Division, Faculty of Engineering, University of Nottingham, University Park, Nottingham NG7 2RD, UK
[b] Materials, Mechanics and Structures Research Division, Faculty of Engineering, University of Nottingham, University Park, Nottingham NG7 2RD, UK

ARTICLE INFO

Article history:
Received 6 October 2010
Received in revised form
14 September 2011
Accepted 30 September 2011
Available online 12 November 2011

Keywords:
Straight-build assembly
Parallelism-build assembly
Tolerance analysis
Monte Carlo simulation
Variation propagation control

ABSTRACT

Variation propagation control is one of the procedures used to improve product quality in the manufacturing assembly process. The quality of a product assembly depends on the product type and the optimization criteria employed in the assembly. This paper presents two assembly procedures of component stacks by controlling variation propagation. The procedures considered are: (i) straight-build assembly by minimizing the distances from the centres of components to table axis; (ii) parallelism-build assembly by minimizing the angular errors between actual and nominal planes. Simulation results are presented for the assembly of four cylindrical components. The results indicate that the variation can be reduced significantly by using these procedures, compared to that without minimization. The results also indicate that the variation not only greatly relies on the assembly procedures, but also on the number of available orientations at the assembly stage. The radial variation increases with the stage for the straight-build assembly, while the angular error decreases with the stage for the parallelism-build assembly. The assembly quality for the two assembly procedures can be improved by increasing the number of orientations. The variation decreases exponentially and monotonically with the number of orientations. The information obtained is useful for manufacturing processes and the assembly modeling.

1. Introduction

Variations always exist due to imperfections in the manufacturing processes and materials, and various other random errors. They cause small deviations in parts from the nominal geometry. These deviations propagate and accumulate as parts are assembled and can quickly drive assembly dimensions out of specification [1–5]. Tolerance assignment in mechanical engineering product design and manufacturing is critical both for product quality and performance, as well as for its manufacturing cost. A tighter tolerance normally requires more extensive manufacturing effort, resulting in a higher manufacturing cost [6].

Improving quality and reducing cycle time and cost are the main objectives for competitive manufacturing today. These objectives can be achieved partially by effectively controlling the variation propagation in manufacturing [7]. The traditional methods for studying assembly tolerance stackup are usually based on engineering experience, worst on worst tolerance analysis (WOW) method [8–11], or the root-sum-square tolerance analysis (RSS) method [6,12,13]. These methods are used frequently in the analysis of a single-dimensional chain, and are not suitable for the analysis of geometrical tolerances in three-dimensional space. Furthermore, these methods do not take into account the practical assembly procedures, resulting in conservative and expensive solutions.

To reduce the costs and minimize the variation propagation, in recent years, some researchers have explored new methods for the variation control. Mease et al. suggest [14] a cost-effective method, selective assembly. This method focuses on the fit between mating parts rather than the absolute dimension of each component. It can be used to achieve high-precision assembly from relatively low-precision components. In this approach, the mating components are measured, sorted by dimension and binned into groups prior to the assembly process. The final product is assembled by selecting the components from appropriate bins to achieve optimal assembly dimensions. There are costs associated with using a larger number of bins. If there are no components of one type in a particular bin at a particular time, the mating components in the corresponding bin cannot be used. Mantripragada and Whitney [1] suggest that the variation propagation is controlled by designing contact features to make adjustments along the assembly process. However, in practice, the contact features are hardly changed in the assembly process. Thus, this paper proposes that the variation is controlled by an effective selection of assembly options. For example, for any rotationally symmetric component assembly, the assembly can be changed by rotating the component about the symmetry axis, and the assembly quality can be improved by a suitable selection of orientations. This would result in either improving

* Corresponding author. Tel.: +44 115 8467683; fax: +44 115 9513800.
E-mail address: zhufang.yang@googlemail.com (Z. Yang).

0278-6125
doi:10.1016/j.jmsy.2011.09.003

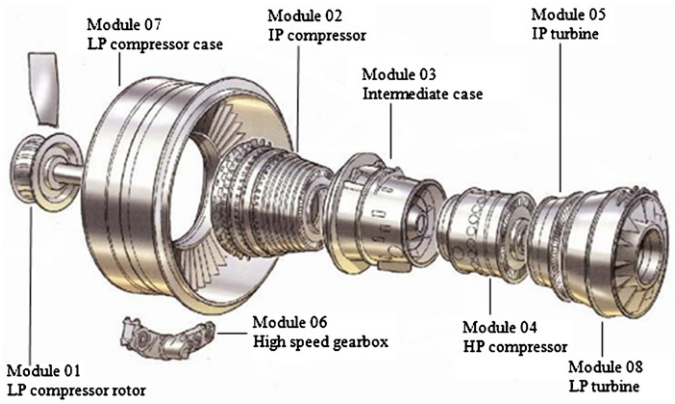

Fig. 1. The modular breakdown of a Trent family engine [22].

the product quality or reducing the manufacturing costs. Therefore, it would be valuable to find out how the available options influence assembly quality. The information obtained would provide significant insight into assembly for manufacturing processes and be useful for the modeling in practical applications. For instance, Rachuri et al. [15] propose a model to capture product assembly information for developing representational methodologies for the next generation of assembly-related standards. The assembly information model requires information regarding parts and their assembly relationships. Shi et al. [16–19] recommend a systematic variation reducing strategy by monitoring process consistency and identifying the variation sources based on available online measurements. This systematic variation reducing strategy involves very complex modeling work, such as components deviation modeling, assembly process modeling, and measurement deviation modeling. This systematic variation reducing strategy also requires information about components deviation and their inter-correlation among different assembly stages. Furthermore, the dimension of systematic variation models increases dramatically with the number of process routes and stages, resulting in heavy computation.

The quality of a product assembly is also greatly dependent on the product type and the optimization techniques employed in the assembly [20,21]. Due to the complexity of a manufacturing process, an effective method for the assembly would be highly desirable [20]. For example, in a multistage radial flow submersible pump assembly, it requires a parallelism-build assembly, and axial play between the impeller and the volute casing is required to have a tolerance of ±0.5 mm, to prevent rubbing action [21]. For the assembly of aero-engine components, such as compressor stages, Module 04 shown in Fig. 1 [22], a precise alignment and clamping device of rotationally symmetric parts is required [23]. The concentricity deviation of the part must be within a 2.5 μm tolerance to meet the strict vibration requirements of the engine [24]. It requires a straight-build assembly where a key characteristic here is to give a 'straight line' between the centres of the parts for the assembly process.

Furthermore, the practical assembly mainly involves cylindrical or/and polyhedral components [25–29]. For example, in the assembly of aero-engine components, all of the parts are cylindrical components, as shown in Fig. 1 [22]. The cylindrical and polyhedral components belong to the same family [30]; once the kinematic parameters within a tolerance range are identified, the results are readily usable for any tolerance specification in the same family. Thus, this paper considers a practical cylindrical-component assembly. For the assembly considered, the variation control usually focuses on minimizing the concentricity deviation and/or axial runout, and these types of variation control will be considered here.

In summary, this paper presents two assembly procedures for controlling variation propagation in the assembly of cylindrical component stacks, as follows:

- Straight-build assembly by minimizing the distances from the centres of components to table axis to control the radial variation, where the radial variation is used as a measure of the quality of straight-build assembly.
- Parallelism-build assembly by minimizing the angular errors between actual and nominal planes to control axial runout, where the angular error is used as a measure of the quality of the parallelism-build assembly.

The minimal variation propagation can be achieved by minimizing the variation stage-by-stage according the assembly process, or by minimizing the sum of squared variations based on all the information for all the assembly stages. The latter is based on ideal conditions without process errors, disturbances etc. in manufacturing processes. However, due to the complexity and randomness of uncertainties and disturbances in manufacturing processes, the minimizing the sum of squared variations for the all assembly stages cannot guarantee the delivery of desired product quality. Thus the paper considers the practical assembly operations to provide an economical and effective solution to analyze tolerance build up. During the assembly, variation propagation is minimized stage-by-stage by rotating the component about its symmetry axis, according to the available number of practical orientations. To validate the two assembly methods, Monte Carlo simulations are performed. The relationship between variation propagation and the number of orientations is also investigated.

Details of the two assembly methods are given in Section 2. A four-cylindrical-component assembly is described in Section 3. The results obtained using the two assembly methods are presented in Section 4, the relationship between variation propagation and the number of orientations is also given in Section 4. The conclusions from the study are presented in Section 5.

2. Two assembly techniques

The proposed assembly techniques are: (i) straight-build assembly and (ii) parallelism-build assembly. Here, the paper uses two cylindrical components to demonstrate the straight-build assembly and parallelism-build assembly, as shown in Figs. 2 and 3, respectively, where C_1 and C_2 are the two component centres at their top ends. The nominal plane is defined by the base of the first component. V_1 and V_2 are normal vectors to the nominal and actual uppermost planes, respectively. The axis normal to the nominal base plane is called "table axis". The techniques are described as follows:

- *Straight-build assembly:* minimize radial variation from the component centre to table axis stage-by-stage, as shown in Fig. 2.
- *Parallelism-build assembly:* minimize angular error between actual and nominal planes stage-by-stage, as shown in Fig. 3.

The two proposed assembly algorithms are developed from state transition models, consisting of three steps: (1) calculating the total differential translational and rotational vectors for a given variation and orientations of the components; (2) calculating of the translational error vector and rotational errors from the differential translational and rotational vectors; and (3) minimizing radial variation or angular errors for the straight-build assembly or parallelism-build assembly from the translational error vector and rotational errors. The calculations for the first two steps are

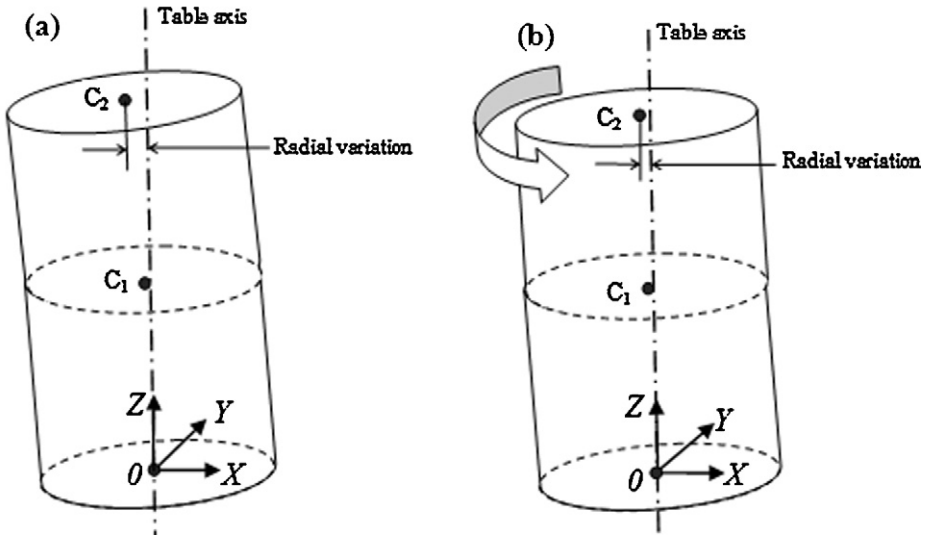

Fig. 2. Straight-build assembly. (a) Without rotating components against each other, (b) with preferred orientations to minimize radial variation.

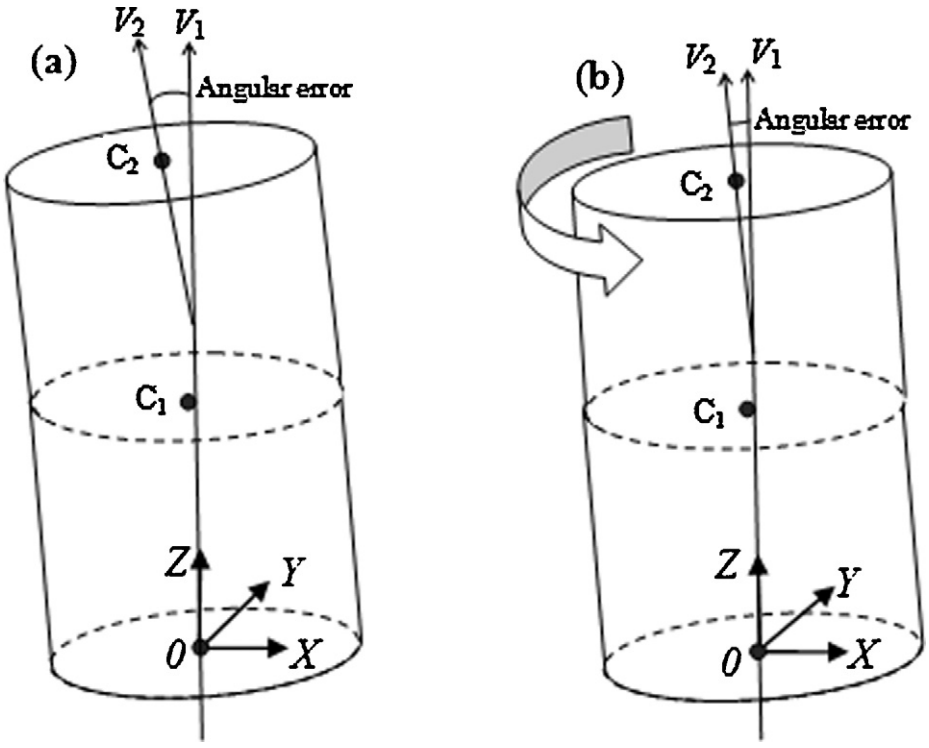

Fig. 3. Parallelism-build assembly. (a) Without rotating components against each other, (b) with preferred orientations to minimize angular error.

given by the developed state transition models in Appendix A. The minimization of radial variation or angular errors for the straight-build assembly or parallelism-build assembly is presented as follows.

2.1. Straight-build assembly algorithm

To minimize radial variation, the second (top) component is rotated about its symmetry axis, and then the translational error vector ($dp_2^x(i)$, $dp_2^y(i)$, $dp_2^z(i)$) is calculated from the state transition models described in Appendix A, according to the available number of practical orientations. The number of orientations is described by rotational matrix R in Eq. (A-3) in Appendix A.

The radial variation for orientation i at Stage 2 is calculated as follows:

$$Radial \quad \mathrm{var}(2,i) = \sqrt{(dp_2^x(i))^2 + (dp_2^y(i))^2} \tag{1}$$

where Stage 2 corresponds to the assembly when the second component is added.

The minimum radial variation for all possible orientations gives the best straight-build assembly at Stage 2 and can be calculated as follows:

$$Radial \quad \mathrm{var}(2) = \min\left\{\sqrt{(dp_2^x(i))^2 + (dp_2^y(i))^2}\right\} \tag{2}$$

where $i = 1,2,\ldots,N$, and N is the maximum number of orientations.

In a similar way, the minimum radial variation at Stage k can be calculated by:

$$Radial \quad \text{var}(k) = \min\left\{\sqrt{(dp_k^x(i))^2 + (dp_k^y(i))^2}\right\} \tag{3}$$

where Stage k corresponds to the assembly when the kth component is added.

Therefore, the minimum radial variation can be obtained at each stage.

2.2. Parallelism-build assembly algorithm

In a similar way, using the state tranistion models described in Appendix A, the rotational errors $(\delta_k^x(i), \delta_k^y(i), \delta_k^z(i))$ can be calculated at each stage for the available orientation i by rotating the component about its symmetry axis, as shown in Fig. 3. The nominal uppermost plane at Stage k is:

$$z = (H_1 + H_2 + \cdots + H_k) \tag{4}$$

where H_i ($i = 1,2,\ldots,k$) is a height of the ith cylindrical component, and k corresponds to the assembly when the kth component is added.

The normal vector to the nominal uppermost plane at Stage k is:

$$V_{k1} = \begin{bmatrix} 0 \\ 0 \\ 1 \end{bmatrix} \tag{5}$$

The normal vector to the actual uppermost plane which has rotational errors $(\delta_k^x(i), \delta_k^y(i), \delta_k^z(i))$ at Stage k is:

$$V_{k2} = \begin{bmatrix} x \\ y \\ z \end{bmatrix} = R_x(\delta_k^x(i))R_y(\delta_k^y(i))R_z(\delta_k^z(i))V_{k1} \tag{6}$$

where

$$R_x(\delta_k^x(i)) = \begin{bmatrix} 1 & 0 & 0 \\ 0 & \cos(\delta_k^x(i)) & -\sin(\delta_k^x(i)) \\ 0 & \sin(\delta_k^x(i)) & \cos(\delta_k^x(i)) \end{bmatrix}, \tag{7}$$

$$R_y(\delta_k^y(i)) = \begin{bmatrix} \cos(\delta_k^y(i)) & 0 & \sin(\delta_k^y(i)) \\ 0 & 1 & 0 \\ -\sin(\delta_k^y(i0) & 0 & \cos(\delta_k^y(i)) \end{bmatrix}, \tag{8}$$

$$R_z(\delta_k^z(i)) = \begin{bmatrix} \cos(\delta_k^z(i)) & -\sin(\delta_k^z(i)) & 0 \\ \sin(\delta_k^z(i)) & \cos(\delta_k^z(i)) & 0 \\ 0 & 0 & 1 \end{bmatrix} \tag{9}$$

Assuming that the rotation angle errors are small, first order small angle approximations have been used such that: $\cos(\delta) \approx 1$, $\sin(\delta) \approx \delta$. Eqs. (7)–(9) can be approximated as follows:

$$R_x(\delta_k^x(i)) \cong \begin{bmatrix} 1 & 0 & 0 \\ 0 & 1 & -\delta_k^x(i) \\ 0 & \delta_k^x(i) & 1 \end{bmatrix}, \tag{10}$$

$$R_y(\delta_k^y(i)) \cong \begin{bmatrix} 1 & 0 & \delta_k^y(i) \\ 0 & 1 & 0 \\ -\delta_k^y(i) & 0 & 1 \end{bmatrix}, \tag{11}$$

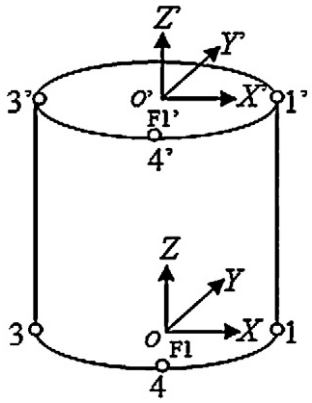

Fig. 4. A cylindrical component.

$$R_z(\delta_k^z(i)) \cong \begin{bmatrix} 1 & -\delta_k^z(i) & 0 \\ \delta_k^z(i) & 1 & 0 \\ 0 & 0 & 1 \end{bmatrix} \tag{12}$$

Substituting Eqs. (5), (10), (11) and (12) into Eq. (6) gives:

$$V_{k2} \cong \begin{bmatrix} \delta_k^y(i) \\ -\delta_k^x(i) \\ 1 \end{bmatrix} \tag{13}$$

The angle $d\theta(k, i)$ between the nominal and actual planes is calculated from the two normal vectors V_{k1} and V_{k2}, such that:

$$\cos(d\theta(k,i)) = \frac{|V_{k1} \cdot V_{k2}|}{|V_{k1}||V_{k2}|} = \frac{1}{\sqrt{(\delta_k^x(i))^2 + (\delta_k^y(i))^2 + 1}} \tag{14}$$

$$d\theta(k,i) = \cos^{-1}\left[\frac{1}{\sqrt{(\delta_k^x(i))^2 + (\delta_k^x(i))^2 + 1}}\right] = \sin^{-1}\left\{\sqrt{\frac{(\delta_k^x(i))^2 + (\delta_k^y(i))^2}{(\delta_k^x(i))^2 + (\delta_k^y(i))^2 + 1}}\right\} \tag{15}$$

where the rotation angle errors (δ_k^x and δ_k^y) are very small compared to 1 and negligible, such that Eq. (15) can be rewritten as

$$d\theta(k,i) \cong \sin^{-1}\left\{\sqrt{(\delta_k^x(i))^2 + (\delta_k^y(i))^2}\right\} \cong \sqrt{(\delta_k^x(i))^2 + (\delta_k^y(i))^2} \tag{16}$$

The minimum angular error for all possible orientations gives the best parallelism-build assembly at Stage k and can be calculated as follows:

$$d\theta(k) = \min\left\{\sqrt{(\delta_k^x(i))^2 + (\delta_k^y(i))^2}\right\} \tag{17}$$

where $i = 1,2,\ldots,N$ and N is the maximum number of orientations.

3. An assembly example of four cylindrical components

To illustrate the two optimization techniques for minimizing uncertainty propagation, a practical four-cylindrical-component assembly is considered. The cylindrical component has a height of H (70 mm) with tolerance $\pm h$, and a diameter of Φ (100 mm) with tolerance $\pm\varphi$, as shown in Fig. 4, where $h = \varphi = 0.1$ mm. In practical, each component has limited orientations, here each component is

assumed to have 4, 8, 16 or 20 possible uniformly arranged orientations. Fig. 4 shows the situation when the component has 4 orientations. To analyze the variation propagation statistically, the errors for the diameter and height of the cylindrical component are assumed to be normally distributed, where the standard deviation (σ) is taken to be one sixth of the tolerance range, i.e. one third of 0.1 mm. Each assembly procedure is simulated 10,000 times using standard Monte Carlo methods. For simplicity, the following assumptions are made for the component with 4 possible orientations.

- The top and base surfaces are flat.
- Frames F1 and F1′ are attached to the assembly features.
- Base centre (0,0,0) is the origin in the world coordinate system.
- Points 1, 2, 3 and 4 are uniformly separated by 90° angle in the *XOY* plane with centre *O*, and lie on the circumference of the cylinder on the *OX* and *OY* axes.
- Frame F1′ related to Frame F1 has a translation of (0,0,*H*) with a translation error of (dx,dy,dz) and an angular error of ($d\theta_x$, $d\theta_y$, $d\theta_z$).
- The top centre *O*′ lies at (dx,dy,$dz+H$) relative to *O*.
- Points 1′, 2′, 3′ and 4′ are uniformly separated by 90° angle on the top surface with centre *O*′, and lie on the circumference of the cylinder on the *O*′*X*′ and *O*′*Y*′ axes.

As the cylindrical component has a height of H with tolerance $\pm h$, and a diameter of Φ with tolerance $\pm\varphi$, the size tolerance zone at the component top is enclosed by two cylinders with a height of $2h$ having a diameter of $\Phi-\varphi$ and a diameter of $\Phi+\varphi$, respectively, as shown in Fig. 5(a). In the size tolerance zone, the following inequities can be obtained.

$$|dx| \le \varphi, \tag{18}$$

$$|dy| \le \varphi, \tag{19}$$

$$\sqrt{dx^2+dy^2} \le \varphi, \tag{20}$$

$$|dz| \le h, \tag{21}$$

$$|d\theta_x| \le \tan^{-1}\left(\frac{h-|dz|}{0.5\Phi}\right), \tag{22}$$

$$|d\theta_y| \le \tan^{-1}\left(\frac{h-|dz|}{0.5\Phi}\right), \tag{23}$$

$$|d\theta_z| \le \tan^{-1}\left(\frac{\varphi-|dy|}{0.5\Phi}\right) \tag{24}$$

Since $(h-|dz|)/0.5\Phi$ and $(\varphi-|dy|)/0.5\Phi$ are very small, the right sides of inequities (22)–(24) can approximately be $(h-|dz|)/0.5\Phi$, $(h-|dz|)/0.5\Phi$ and $(\varphi-|dy|)/0.5\Phi$, respectively. Inequities (22)–(24) can be written as:

$$|d\theta_x| \le \frac{h-|dz|}{0.5\Phi}, \tag{25}$$

$$|d\theta_y| \le \frac{h-|dz|}{0.5\Phi}, \tag{26}$$

$$|d\theta_z| \le \frac{\varphi-|dy|}{0.5\Phi} \tag{27}$$

From inequities (21) and (25), $d\theta_x$ and dz are constrained to lie within the shaded "bounded" region shown in Fig. 5(b). Similarly, from inequities (21) and (26), $d\theta_y$ and dz are constrained to lie within the same shaded "bounded" region as $d\theta_x$ and dz; from inequities (19) and (27), the constrained bounds for $d\theta_z$ and dy can be constructed as shown in Fig. 5(c); and from inequities (18)–(20), the constrained bounds for dx and dy can be constructed as shown in Fig. 5(d). The dx and dz are normally distributed. Each of the variables is randomly and normally generated, and then the second variable generated is limited to the range left by the first one. For example, in Fig. 5(d), if the variable dx is generated first, then

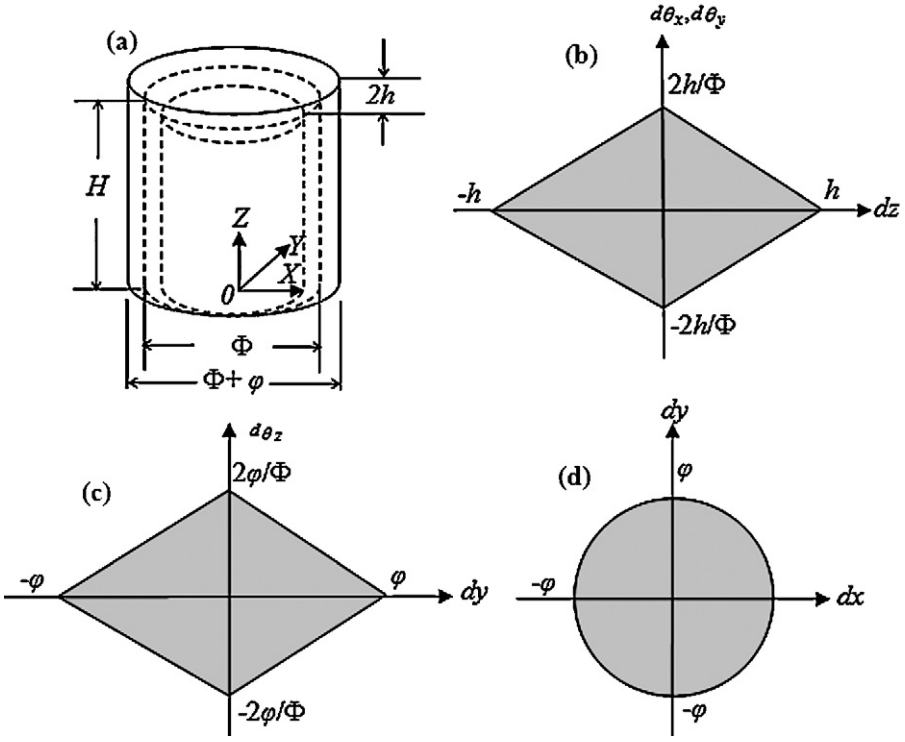

Fig. 5. A size tolerance zone and the bounds used to specify the kinematic parameter space. (a) A size tolerance zone, (b)–(d) define the constrained regions.

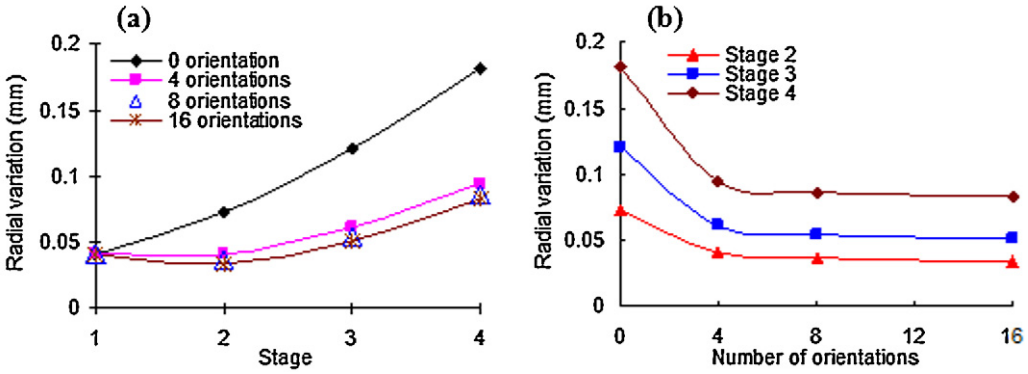

Fig. 6. Variation propagation from the table axis against stage and the number of orientations, respectively. (a) Variation against stage, (b) variation against the number of orientations.

the variable *dy* will be limited to the shaded circled region left by the *dx*. Any instances generated outside $[-3\sigma, +3\sigma]$ are disregarded to respect the shaded "bounded" regions, where the standard deviation is described by σ. Details of the generated variables can be found in [31].

In a similar way, for component with different orientations, similar assumptions as described above can be made and will not be reiterated here.

4. Results and discussion

4.1. Influence of orientations on variation propagation

For the straight-build assembly, the radial variation propagation from the table axis is calculated using Eq. (3). This paper only gives details for the orientations 0, 4, 8 and 16, since the results for 16 orientations are very similar to those for 20 orientations. The average stage-by-stage radial variation against stage from the table axis is shown in Fig. 6(a). The average stage-by-stage radial variation against the number of available orientations from the table axis for Stages 2–4 is shown in Fig. 6(b). The mean and standard deviations of the variations are provided in Table 1, together with the maximum and minimum values. The histograms of the radial variations for 0, 4, 8 and 16 orientations are shown in Fig. 7.

For the parallelism-build assembly, the angular error is calculated using Eq. (17). In a similar way, the paper only gives the results for 0, 4, 8 and 16 orientations. The average angular error is shown in Fig. 8. The mean and standard deviations of the errors are provided in Table 2, together with the maximum and minimum values. The histograms of the angular errors for each procedure are shown in Fig. 9.

To compare the two assembly procedures, angular error for the straight-build assembly and radial variation for the parallelism-build assembly are also calculated, and are given in Section 4.2 below.

All of the results indicate that the error propagation varies significantly with the assembly procedures and the number of orientations.

4.1.1. Influence of orientations on variation propagation for straight-build assembly

From Fig. 6 and Table 1, the average radial variations tend to increase with the stage for the different number of orientations – there is a slight decrease between Stages 1 and 2, where the number of orientations are equal to or more than 4, as shown in Fig. 6(a). The average radial variations decrease with the number of orientations for the same stage, as shown in Fig. 6(b). The results illustrate that the variation propagation can be reduced by increasing the number of orientations. It can be seen that the variation propagation is significantly reduced from 0 to 4 orientations. However, as the number of orientations increases, the variation continues to decrease, but at a less significant rate. For example, the variation at the final stage is reduced by 48% from 0 to 4 orientations, by 10% from 4 to 8 orientations, and by 3% from 8 to 16 orientations. In Fig. 6(b), it is seen that the variation propagation decreases exponentially, rather than proportionally to the number of orientations. This indicates that there is limit to how much the variation can be reduced. It also means that the minimum variation can be achieved at reduced cost by properly selecting the number of orientations.

From Table 1, it is found that the standard deviation of radial variation increases with the stage as well. This indicates that the consistency of the straight-build assembly will decrease with the stage. It is also found that the standard deviation of radial variation decreases significantly from 0 to 4 orientations; while as the number of orientations increases, the standard deviation of radial variation is comparable to that with 4 orientations. This shows that the straight-build assembly has a good consistency with the number of orientations.

From Fig. 7(a)–(d), the procedure with 16 orientations produces the smallest levels of radial variation, with most values occurring in the range 0–0.1 mm. These results further demonstrate that the assembly quality and consistency increase with the number of orientations for the straight-build assembly.

4.1.2. Influence of orientations on variation propagation for parallelism-build assembly

From Fig. 8 and Table 2, the average angular error increases with the stage in the absence of orientations, while it decreases monotonically with stage in the presence of orientations. It also shows that the orientations can significantly reduce the angular error for the parallelism-build assembly, compared to the assembly without orientations. For example, the angular error at the final stage is reduced by 63% from 0 to 4 orientations. However, as the number of orientations increases, the angular error continues to decrease, but at a lower rate. For example, the angular error at the final stage is reduced by 7.4% from 4 to 8 orientations, and by 2% from 8 to 16 orientations. From Fig. 8(b), the angular error propagation appears to decrease exponentially, rather than proportionally to the number of orientations, as described earlier for straight-build assembly. This also indicates that there is a limitation on reducing the angular error, and a proper selection of the number of orientations can achieve the minimum angular error with reduced cost.

Table 2 indicates that the standard deviation of the angular error increases with stage without orientations, while it is smaller in the presence of orientations. These results confirm that the parallelism-build assembly can be improved by using the orientations.

Table 1
Radial variation propagation from the table axis for straight-build assembly.

Number of orientations	Stage	Max variation (mm)	Min variation (mm)	Average variation (mm)	Standard deviation of variation (mm)
0	1	0.0999	4.0078×10^{-4}	0.0412	0.0208
	2	0.2481	7.7686×10^{-4}	0.0727	0.0380
	3	0.4434	0.0018	0.1198	0.0643
	4	0.6599	5.9583×10^{-4}	0.1813	0.0978
4	1	0.0999	4.0078×10^{-4}	0.0412	0.0208
	2	0.1782	3.3417×10^{-4}	0.0405	0.0249
	3	0.3069	6.1712×10^{-4}	0.0605	0.0439
	4	0.5117	3.4981×10^{-4}	0.0946	0.0726
8	1	0.0999	4.0078×10^{-4}	0.0412	0.0208
	2	0.1782	3.3417×10^{-4}	0.0356	0.0253
	3	0.3069	2.6078×10^{-4}	0.0535	0.0436
	4	0.5220	7.0305×10^{-4}	0.0856	0.0721
16	1	0.0999	4.0078×10^{-4}	0.0412	0.0208
	2	0.1782	3.3417×10^{-4}	0.0338	0.0259
	3	0.2981	3.8648×10^{-4}	0.0513	0.0440
	4	0.5120	2.1112×10^{-4}	0.0829	0.0723
20	1	0.0999	4.0078×10^{-4}	0.0412	0.0208
	2	0.1782	2.7312×10^{-4}	0.0335	0.0260
	3	0.3000	1.0063×10^{-4}	0.0510	0.0441
	4	0.5130	2.8536×10^{-4}	0.0825	0.0724

From Fig. 9(a)–(d), the parallelism-build assembly with 16 orientations produces the smallest levels of angular error, with most values occurring in the range 0–0.001 rad. These results further demonstrate that a proper selection of the number of orientations can minimize the angular error at reduced cost for the parallelism-build assembly.

In summary, the average radial variation increases with stage for the straight-build assembly, while the average angular error decreases with stage for the parallelism-build assembly in the presence of orientations. The statistical results above indicate that the quality of the two assembly procedures can be improved by increasing the number of orientations.

4.2. Discussion

As mentioned earlier, to compare the two assembly procedures and study the effect of using different number of orientations on the error propagation, the radial variation for parallelism-build

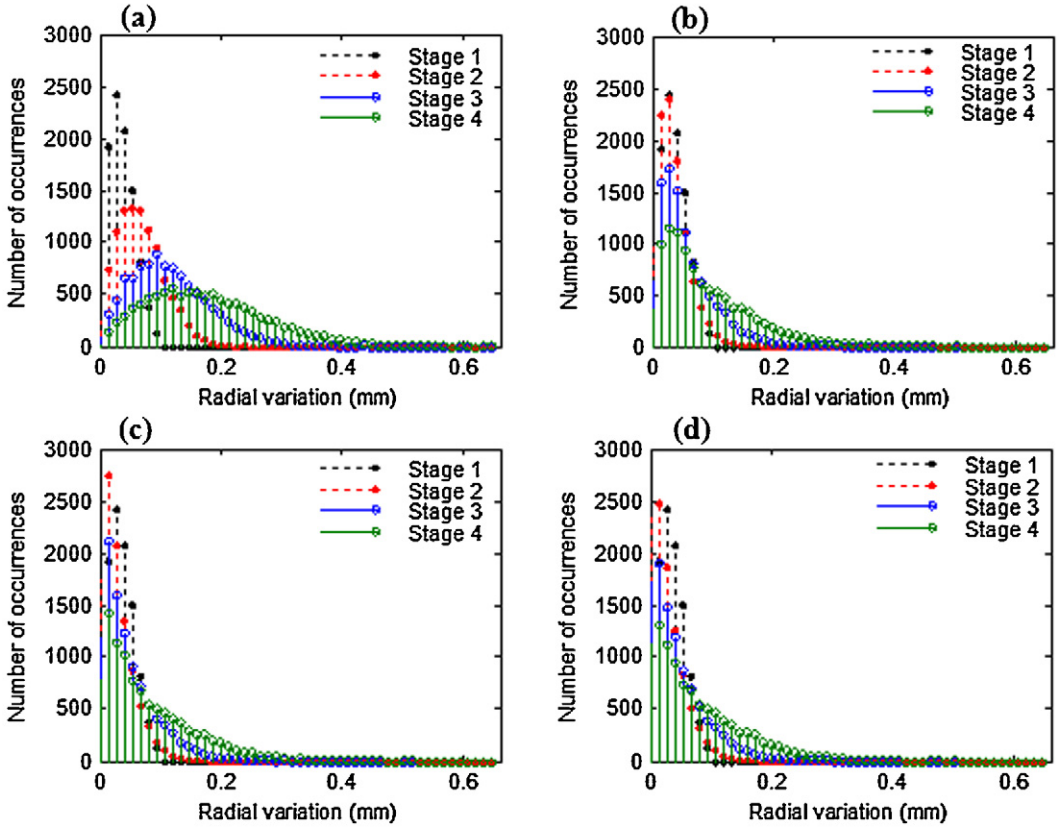

Fig. 7. Histogram of variation propagation from the table axis. (a) 0 orientation, (b) 4 orientations, (c) 8 orientations, (d) 16 orientations.

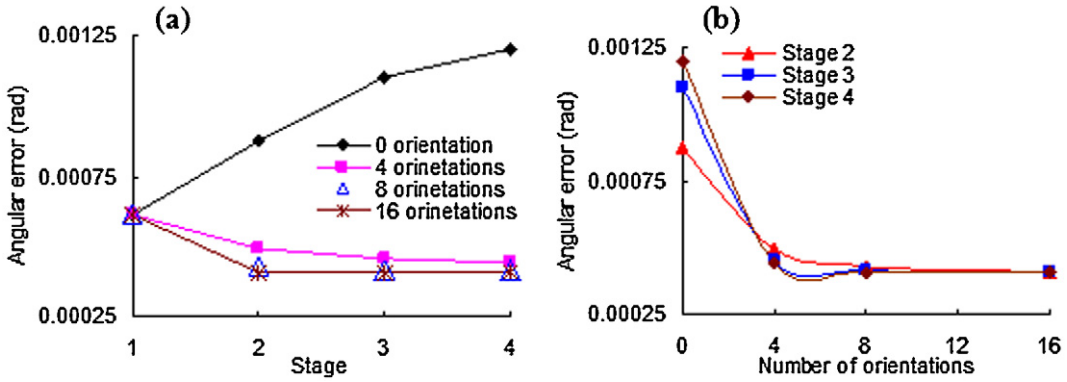

Fig. 8. Angular error against stage and the number of orientations, respectively. (a) Variation against stage, (b) angular error against the number of orientations.

Table 2
Angular error for parallelism-build assembly.

Number of orientations	Stage	Max error (rad)	Min error (rad)	Average error (rad)	Standard deviation of error (rad)
0	1	0.0020	3.6311×10^{-7}	6.0901×10^{-4}	3.5427×10^{-4}
	2	0.0030	4.2030×10^{-6}	8.7466×10^{-4}	4.7417×10^{-4}
	3	0.0044	1.8471×10^{-5}	0.0011	5.7669×10^{-4}
	4	0.0045	1.0520×10^{-5}	0.0012	6.6198×10^{-4}
4	1	0.0020	3.6311×10^{-7}	6.0901×10^{-4}	3.5427×10^{-4}
	2	0.0018	4.2030×10^{-6}	4.9176×10^{-4}	2.9455×10^{-4}
	3	0.0018	4.1063×10^{-6}	4.5436×10^{-4}	2.8031×10^{-4}
	4	0.0018	5.4738×10^{-6}	4.4375×10^{-4}	2.8361×10^{-4}
8	1	0.0020	3.6311×10^{-7}	6.0901×10^{-4}	3.5427×10^{-4}
	2	0.0018	4.2030×10^{-6}	4.2856×10^{-4}	2.9585×10^{-4}
	3	0.0018	3.3571×10^{-6}	4.1259×10^{-4}	2.9617×10^{-4}
	4	0.0018	1.1027×10^{-6}	4.1099×10^{-4}	2.9763×10^{-4}
16	1	0.0020	3.6311×10^{-7}	6.0901×10^{-4}	3.5427×10^{-4}
	2	0.0018	2.1714×10^{-6}	4.0784×10^{-4}	3.0243×10^{-4}
	3	0.0019	1.8242×10^{-6}	4.0658×10^{-4}	3.0686×10^{-4}
	4	0.0018	2.8310×10^{-6}	4.0276×10^{-4}	3.0723×10^{-4}
20	1	0.0020	3.6311×10^{-7}	6.0901×10^{-4}	3.5427×10^{-4}
	2	0.0018	6.6695×10^{-7}	4.0415×10^{-4}	3.0435×10^{-4}
	3	0.0019	1.7187×10^{-6}	4.0651×10^{-4}	3.0917×10^{-4}
	4	0.0018	4.9368×10^{-7}	4.0146×10^{-4}	3.0913×10^{-4}

Table 3
Radial variation propagation from the table axis for the different assembly procedures.

Procedure	Stage	Max variation (mm)	Min variation (mm)	Average variation (mm)	Standard deviation of variation (mm)
Straight-build assembly	1	0.0999	4.0078×10^{-4}	0.0412	0.0208
	2	0.1782	3.3417×10^{-4}	0.0405	0.0249
	3	0.3069	6.1712×10^{-4}	0.0605	0.0439
	4	0.5117	3.4981×10^{-4}	0.0946	0.0726
Parallelism-build assembly	1	0.0999	4.0078×10^{-4}	0.0412	0.0208
	2	0.2589	3.3417×10^{-4}	0.0721	0.0376
	3	0.3343	9.6801×10^{-4}	0.0949	0.0529
	4	0.4487	3.4981×10^{-4}	0.1109	0.0626

Table 4
Angular error for the different assembly procedures.

Procedure	Stage	Max error (rad)	Min error (rad)	Average error (rad)	Standard deviation of error (rad)
Straight-build assembly	1	0.0020	3.6311×10^{-7}	6.0901×10^{-4}	3.5427×10^{-4}
	2	0.0030	4.2030×10^{-6}	8.7187×10^{-4}	4.7413×10^{-4}
	3	0.0039	1.8941×10^{-5}	0.0011	5.7701×10^{-4}
	4	0.0047	9.4271×10^{-6}	0.0012	6.6464×10^{-4}
Parallelism-build assembly	1	0.0020	3.6311×10^{-7}	6.0901×10^{-4}	3.5427×10^{-4}
	2	0.0018	4.2030×10^{-6}	4.9176×10^{-4}	2.9455×10^{-4}
	3	0.0018	4.1063×10^{-6}	4.5436×10^{-4}	2.8031×10^{-4}
	4	0.0018	5.4738×10^{-6}	4.4375×10^{-4}	2.8361×10^{-4}

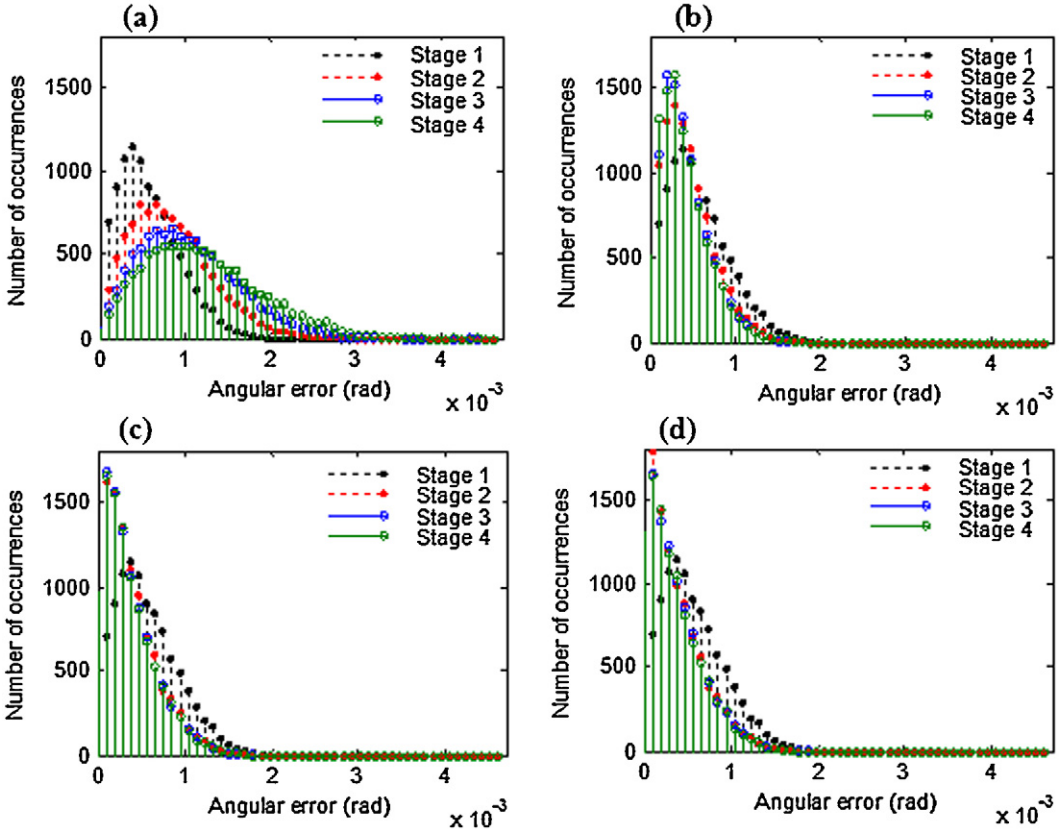

Fig. 9. Histogram of angular error. (a) 0 orientation, (b) 4 orientations, (c) 8 orientations, (d) 16 orientations.

assembly and angular error for straight-build assembly are calculated. The results have a similar pattern for the different orientations and are only shown for components with 4 orientations. Comparisons of average radial variation and angular error are shown in Fig. 10(a) and (b), respectively, for the different assembly procedures. The mean and standard deviations of the variations and angular error are provided in Tables 3 and 4, together with the maximum and minimum values, for parallelism-build assembly and straight-build assembly, respectively. The histograms of the radial variations and angular error for parallelism-build assembly and straight-build assembly are shown in Fig. 11(a) and (b), respectively.

From Fig. 10, it is seen that the straight-build assembly has smaller radial variation than the parallelism-build assembly from the table-axis, while the parallelism-build assembly provides reduced angular error, compared to the straight-build assembly. It is very interesting to notice that the radial variation increases rapidly after Stage 2 for the straight-build assembly, but the radial variation changes much more gently for the parallelism-build assembly, as shown in Fig. 10(a). This indicates that the minimal radial variation could be achieved by constraining the angular error in the straight-build assembly. Further studies to investigate this are under way, and will be reported at a later date.

From Table 3, the parallelism-build assembly has higher radial variation propagation; for example, the radial variation in the parallelism-build assembly is increased by 17% at Stage 4, compared to the straight-build assembly. Figs. 11(a) and 6(b) further demonstrate that the parallelism-build assembly increases radial variation propagation, where most values of the radial variation occurs in the range 0–0.1 mm for the straight-build assembly and in the range 0–0.15 mm for the parallelism-build assembly, respectively.

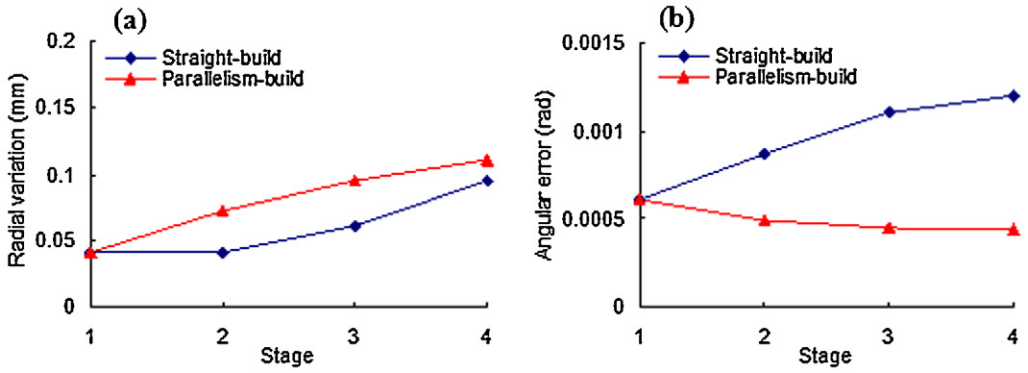

Fig. 10. Radial variation and angular error for the different assembly procedures. (a) Radial variation, (b) angular error.

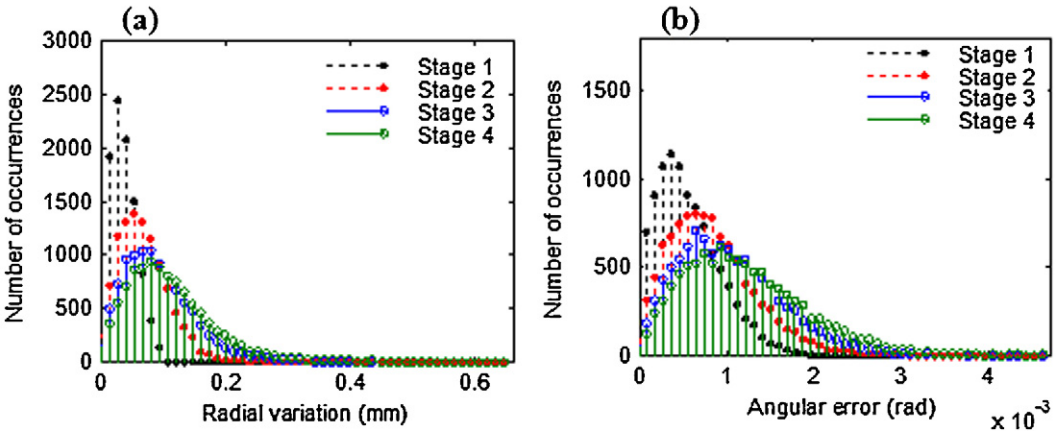

Fig. 11. Histograms of radial variation for parallelism-build assembly and angular error for straight-build assembly. (a) Radial variation for parallelism-build assembly, (b) angular error for straight-build assembly.

From Table 4, the parallelism-build assembly gives much lower angular error than the straight-build assembly. For instance, the angular error in the parallelism-build assembly is reduced by 63% at Stage 4, compared to the straight-build assembly. From Figs. 9(b) and 11(b), the parallelism-build assembly in the presence of orientations produces smaller levels of angular error, with most values occurring in the range 0–0.001 rad; while most values of angular error occur in the range 0–0.002 rad for the straight-build assembly. This indicates that the assembly procedure needs to be selected carefully in accordance with the particular industrial application.

From the average radial variations for the component with 4 orientations in Fig. 10(a), and with 0 orientation in Fig. 6(a), it is interesting to notice that not only the straight-build assembly but also the parallelism-build assembly can have reduced radial variation with orientations, the radial variation is reduced by 48% and 39% in the straight-build assembly and the parallelism-build assembly, respectively, compared to the procedure without orientations. This indicates that the orientations can improve the assembly quality.

5. Conclusions

Two assembly methods, straight-build assembly and parallelism-build assembly, have been analyzed for different number of orientations. The average radial variations and angular errors decrease with the number of available orientations for the same stage. The simulation results obtained indicate that the two assembly methods have the potential to significantly reduce manufacturing assembly errors. For the example considered, the first method reduces the radial variation by 48%, whist the second the angular error by 63%, where the component has 4 orientations, when compared to assemblies without orientations.

The straight-build assembly produces the minimum radial variation; and the parallelism-build assembly has the minimum angular error. For the first method, the average radial variations tend to increase with the stage for the different number of orientations; however, for the second method, the average angular error increases with the stage in the absence of orientations, while it decreases with the stage in the presence of orientations.

The two assembly methods have a good consistency, for instance, the maximum standard deviation is 0.0726 mm in the first method, and 3.5×10^{-4} rad in the second method in the presence of orientations.

The variation not only depends on the assembly procedures, but also on the number of orientations. The variation propagation decreases monotonously and exponentially with the number of orientations. Assembly quality could be improved by increasing number of orientations, however, the variation reduction is limited when the number of orientations becomes larger. Therefore, the best assembly and minimal manufacturing cost could be achieved by optimizing the selection of the number of orientations and assembly procedures.

The procedure of the two assembly methods is very simple, and can be easily used to analyze the variation propagation in manufacturing processes.

Acknowledgements

The authors gratefully acknowledge financial support from the Engineering and Physical Sciences Research Council through NIMRC project for this work. The authors also gratefully acknowledge help and advice from Mat Yates and Steve Slack at Rolls-Royce plc.

Appendix A. State transition models

The state transition models are developed from robot manipulator [32], and consist of (i) modeling individual frame errors, (ii) total differential translation and rotation transformation, and (iii) calculation of Cartesian position and orientation errors in the world coordinate. The models are slightly different from those developed by Mantripragada and Whitney [1,33]. Since the variation in the world coordinates system is not only related to the differential rotation and translation in individual frame, but also dependent on nominal orientation and transition relative to the world coordinates system, the differential rotation and translation in individual frame must be converted into those in the world coordinates system through the transformation with respect to the world coordinates system, so that the variation is allowed to be the sum of those differential rotations and translations in the world coordinates system. However, Mantripragada and Whitney's models regard relative transformation of two consecutive frames as that in the world coordinates system, and convert the differential position and orientation vectors in individual frame into the world coordinates system through the relative transformation. Their models of the variation propagation based on the wrong conversion cannot handle the misorientation and misposition of the components. Therefore, this paper presents a detailed derivation of the state transition models. The corrections of Mantripragada and Whitney's models are also given in Appendix A.2 below.

A.1. Modeling individual frame errors

Any manipulator can be considered to consist of a series of links connected together by joints. A coordinate frame can be embedded in each link of the manipulator, and then the relative position and orientation between these coordinate frames can be described by using homogeneous transformations [33]. The homogeneous transformation describing the relation between one link and the next has been called an A matrix [34]. An A matrix is simply a homogeneous transformation describing the relative translation and rotation between link coordinate systems. For example, A_1 describes the position and orientation of the first link. A_2 describes the position and orientation of the second link with respect to the first. Thus the position and orientation of the second in the base coordinates are given by the matrix product.

$$T_2 = A_1 A_2 \tag{A-1}$$

Similarly, A_i describes the ith link in terms of the $(i-1)$, the position and orientation of the ith link relative to the base coordinates are given by the matrix product as follows [32,35]:

$$T_i = A_1 A_2 \ldots A_i = \begin{bmatrix} R_i & p_i \\ 0 & 1 \end{bmatrix} \tag{A-2}$$

where $i = 1,2,\ldots,N$, R_i is the rotational matrix, p_i is the positional vector, $A_i = (A_i)_{Trans}(A_i)_{RotX}(A_i)_{RotY}(A_i)_{RotZ}$,

$$(A_i)_{Trans} = \begin{bmatrix} 1 & 0 & 0 & X_i \\ 0 & 1 & 0 & Y_i \\ 0 & 0 & 1 & Z_i \\ 0 & 0 & 0 & 1 \end{bmatrix},$$

$$(A_i)_{RotX} = \begin{bmatrix} 1 & 0 & 0 & 0 \\ 0 & \cos(x_i) & -\sin(x_i) & 0 \\ 0 & \sin(x_i) & \cos(x_i) & 0 \\ 0 & 0 & 0 & 1 \end{bmatrix},$$

$$(A_i)_{RotY} = \begin{bmatrix} \cos(y_i) & 0 & \sin(y_i) & 0 \\ 0 & 1 & 0 & 0 \\ -\sin(y_i) & 0 & \cos(y_i) & 0 \\ 0 & 0 & 0 & 1 \end{bmatrix},$$

$$(A_i)_{RotZ} = \begin{bmatrix} \cos(z_i) & -\sin(z_i) & 0 & 0 \\ \sin(z_i) & \cos(z_i) & 0 & 0 \\ 0 & 0 & 1 & 0 \\ 0 & 0 & 0 & 1 \end{bmatrix},$$

X_i, Y_i and Z_i are the displacements along the x-, y- and z-axes between frames i and $i-1$. x_i, y_i and z_i are the angles between frames i and $i-1$ rotating about x-, y- and z-axes, respectively.

Thus T_i represents the position and orientation of frame i with respect to the world coordinates, if the base coordinates are assumed to be the world coordinates, as described in [35,36].

The homogeneous transformation matrix A_i can be rewritten as:

$$A_i = \begin{bmatrix} \cos(y_i)\ \cos(z_i) & -\cos(y_i)\sin(z_i) & \sin(y_i) & X_i \\ \sin(x_i)\ \sin(y_i)\cos(z_i) + \cos(x_i)\sin(z_i) & \cos(x_i)\cos(z_i) - \sin(x_i)\sin(y_i)\sin(z_i) & -\sin(x_i)\cos(y_i) & Y_i \\ \sin(x_i)\sin(z_i) - \cos(x_i)\sin(y_i)\cos(z_i) & \cos(x_i)\sin(y_i)\sin(z_i) + \sin(x_i)\cos(z_i) & \cos(x_i)\cos(y_i) & Z_i \\ 0 & 0 & 0 & 1 \end{bmatrix} \equiv \begin{bmatrix} R_i^- & p_i^- \\ 0T & 1 \end{bmatrix} \tag{A-3}$$

If there are errors in the dimensional relationships between two consecutive coordinate frames, there will be a differential change dA_i between the two coordinate frames, and the correct relation between the two coordinates will be equal to

$$A_i^c = A_i + dA_i \tag{A-4}$$

where A_i is the relationship between the frame coordinates $i-1$ and i, and dA_i is the differential change in their relationship.

The differential change dAi is estimated by the following linear form.

$$dA_i = \frac{\partial A_i}{\partial X_i}\Delta X_i + \frac{\partial A_i}{\partial Y_i}\Delta Y_i + \frac{\partial A_i}{\partial Z_i}\Delta Z_i + \frac{\partial A_i}{\partial x_i}\Delta x_i + \frac{\partial A_i}{\partial y_i}\Delta y_i + \frac{\partial A_i}{\partial z_i}\Delta z_i \tag{A-5}$$

where ΔX_i, ΔY_i, ΔZ_i, Δx_i, Δy_i and Δz_i are small errors in the kinematic parameters.

If δA_i is defined as an error matrix transform with respect to frame $i-1$, the following equations can be obtained.

$$dA_i = \delta A_i * A_i \tag{A-6}$$

$$\delta A_i = D_X \Delta X_i + D_Y \Delta Y_i + D_Z \Delta Z_i + D_x \Delta x_i + D_y \Delta y_i + D_z \Delta z_i \tag{A-7}$$

The D matrices are defined as follows:

$$D_X = \left(\frac{\partial A_i}{\partial X_i}\right) Ai - 1, \quad D_Y = \left(\frac{\partial A_i}{\partial Y_i}\right) A_i^{-1}, \quad D_Z = \left(\frac{\partial A_i}{\partial Z_i}\right) A_i^{-1},$$

$$D_x = \left(\frac{\partial A_i}{\partial x_i}\right) A_i^{-1}, \quad D_y = \left(\frac{\partial A_i}{\partial y_i}\right) A_i^{-1}, \quad D_y = \left(\frac{\partial A_i}{\partial z_i}\right) A_i^{-1}$$

Then

$$D_X = \begin{bmatrix} 0 & 0 & 0 & 1 \\ 0 & 0 & 0 & 0 \\ 0 & 0 & 0 & 0 \\ 0 & 0 & 0 & 0 \end{bmatrix}, \quad D_Y = \begin{bmatrix} 0 & 0 & 0 & 0 \\ 0 & 0 & 0 & 1 \\ 0 & 0 & 0 & 0 \\ 0 & 0 & 0 & 0 \end{bmatrix},$$

$$D_Z = \begin{bmatrix} 0 & 0 & 0 & 0 \\ 0 & 0 & 0 & 0 \\ 0 & 0 & 0 & 1 \\ 0 & 0 & 0 & 0 \end{bmatrix} \tag{A-8}$$

$$D_x = \begin{bmatrix} 0 & 0 & 0 & 0 \\ 0 & 0 & -1 & Z_i \\ 0 & 1 & 0 & -Y_i \\ 0 & 0 & 0 & 0 \end{bmatrix} \tag{A-9}$$

$$D_y = \begin{bmatrix} 0 & -\sin(x_i) & \cos(x_i) & Y_i\ \sin(x_i) - Z_i\cos(x_i) \\ \sin(x_i) & 0 & 0 & -X_i\ \sin(x_i) \\ -\cos(x_i) & 0 & 0 & X_i\ \cos(x_i) \\ 0 & 0 & 0 & 0 \end{bmatrix} \quad \text{(A-10)}$$

$$D_z = \begin{bmatrix} 0 & -\cos(x_i)\cos(y_i) & -\sin(x_i)\cos(y_i) & Y_i\cos(x_i)\cos(y_i) + Z_i\sin(x_i)\cos(y_i) \\ \cos(x_i)\cos(y_i) & 0 & -\sin(y_i) & -X_i\cos(x_i)\cos(y_i) + Z_i\sin(y_i) \\ \sin(x_i)\cos(y_i) & \sin(y_i) & 0 & -X_i\sin(x_i)\cos(y_i) - Y_i\sin(y_i) \\ 0 & 0 & 0 & 0 \end{bmatrix} \quad \text{(A-11)}$$

Eq. (A-7) can be rewritten as

$$\begin{aligned} \delta A_i &= D_X\Delta X_i + D_Y\Delta Y_i + D_Z\Delta Z_i + D_x\Delta x_i + D_y\Delta y_i + D_z\Delta z_i \\ &= \begin{bmatrix} \delta R_i & d_i \\ 0 & 0 \end{bmatrix} = \begin{bmatrix} 0 & -\delta z_i & \delta y_i & dx_i \\ \delta z_i & 0 & -\delta x_i & dy_i \\ -\delta y_i & \delta x_i & 0 & dz_i \\ 0 & 0 & 0 & 0 \end{bmatrix} \end{aligned} \quad \text{(A-12)}$$

From Eqs. (A-8)–(A-12), the following equations can be obtained:

$$d_i = \begin{bmatrix} dx_i \\ dy_i \\ dz_i \end{bmatrix} = \begin{bmatrix} 1 \\ 0 \\ 0 \end{bmatrix}\Delta X_i + \begin{bmatrix} 0 \\ 1 \\ 0 \end{bmatrix}\Delta Y_i + \begin{bmatrix} 0 \\ 0 \\ 1 \end{bmatrix}\Delta Z_i + \begin{bmatrix} 0 \\ Z_i \\ -Y_i \end{bmatrix}$$

$$\Delta x_i + \begin{bmatrix} Y_i\ \sin(x_i) - Z_i\cos(x_i) \\ -X_i\sin(x_i) \\ X_i\cos(x_i) \end{bmatrix}$$

$$\Delta y_i + \begin{bmatrix} [Y_i\cos(x_i) + Z_i\sin(x_i)]\cos(y_i) \\ -X_i\ \cos(x_i)\cos(y_i) + Z_i\sin(y_i) \\ -X_i\sin(x_i)\cos(y_i) - Y_i\sin(y_i) \end{bmatrix}\Delta z_i \quad \text{(A-13)}$$

$$\delta i = \begin{bmatrix} \delta x_i \\ \delta y_i \\ \delta z_i \end{bmatrix} = \begin{bmatrix} 1 \\ 0 \\ 0 \end{bmatrix}\Delta x_i + \begin{bmatrix} 0 \\ \cos(x_i) \\ \sin(x_i) \end{bmatrix}$$

$$\Delta y_i + \begin{bmatrix} \sin(y_i) \\ -\sin(x_i)\ \cos(y_i) \\ \cos(x_i)\cos(y_i) \end{bmatrix}\Delta z_i \quad \text{(A-14)}$$

Eqs. (A-13) and (A-14) can be rewritten as Eqs. (A-15) and (A-16), respectively.

$$d_i = m_{1i}\Delta X_i + m_{2i}\Delta Y_i + m_{3i}\Delta Z_i + m_{4i}\Delta x_i + m_{5i}\Delta y_i + m_{6i}\Delta x_i \quad \text{(A-15)}$$

$$\delta_i = m_{7i}\Delta x_i + m_{8i}\Delta y_i + m_{9i}\Delta z_i \quad \text{(A-16)}$$

where

$$m_{1i} = \begin{bmatrix} 1 \\ 0 \\ 0 \end{bmatrix}, \quad m_{2i} = \begin{bmatrix} 0 \\ 1 \\ 0 \end{bmatrix}, \quad m_{3i} = \begin{bmatrix} 0 \\ 0 \\ 1 \end{bmatrix}, \quad m_{4i} = \begin{bmatrix} 0 \\ Z_i \\ -Y_i \end{bmatrix},$$

$$m_{5i} = \begin{bmatrix} Y_i\sin(x_i) - Z_i\cos(x_i) \\ -X_i\sin(x_i) \\ X_i\cos(x_i) \end{bmatrix},$$

$$m_{6i} = \begin{bmatrix} [Y_i\cos(x_i) + Z_i\sin(x_i)]\cos(y_i) \\ -X_i\ \cos(x_i)\cos(y_i) + Z_i\sin(y_i) \\ -X_i\sin(x_i)\cos(y_i) - Y_i\sin(y_i) \end{bmatrix}, \quad m_{7i} = \begin{bmatrix} 1 \\ 0 \\ 0 \end{bmatrix},$$

$$m_{8i} = \begin{bmatrix} 0 \\ \cos(x_i) \\ \sin(x_i) \end{bmatrix} \quad \text{and} \quad m_{9i} = \begin{bmatrix} \sin(y_i) \\ -\sin(x_i)\ \cos(y_i) \\ \cos(x_i)\cos(y_i) \end{bmatrix}$$

A.2. Total differential translation and rotation transformation

The transformation from the end to the base frames for N frames can be expressed as:

$$T_N + dT_N = \sum_{i=1}^{N}(A_i + dA_i) \quad \text{(A-17)}$$

where dT_N represents the total differential change due to the kinematic errors.

By expanding Eq. (A-17), and ignoring the higher order differential changes, the following linear result is obtained.

$$T_N + dT_N = T_N + \sum_{i=1}^{N}(A_1\cdots A_{i-1}dA_iA_{i+1}\cdots A_N) \quad \text{(A-18)}$$

Substituting Eq. (A-6) into Eq. (A-18) gives

$$dT_N = \sum_{i=1}^{N}(A_1\cdots A_{i-1}\delta A_iA_iA_{i+1}\cdots A_N) \quad \text{(A-19)}$$

Using the definition of T_{i-1} in Eq. (A-2), Eq. (A-19) can be expressed as

$$dT_N = \sum_{i=1}^{N}(T_{i-1})\delta A_iT_{i-1}^{-1}T_N) \quad \text{(A-20)}$$

By defining an error matrix transform δT_N^w with respect to the world coordinates

$$dT_N = \delta T_N^w T_N \tag{A-21}$$

and

$$\delta T_N^w = \begin{bmatrix} 0 & -\delta z_N^w & \delta y_N^w & dx_N^w \\ \delta z_N^w & 0 & -\delta x_N^w & dy_N^w \\ -\delta y_N^w & \delta x_N^w & 0 & dz_N^w \\ 0 & 0 & 0 & 0 \end{bmatrix} \tag{A-22}$$

Then Eq. (A-20) can be rewritten as:

$$\delta T_N^w = \sum_{i=1}^{N} (T_{i-1} \delta A_i T_{i-1}^{-1}) \tag{A-23}$$

From Eqs. (A-3), (A-22) and (A-23), the combined vectors d_N^w and δ_N^w associated with the total transformation of N frames can be calculated as:

$$\begin{aligned} d_N^w &= \sum_{i=1}^{N} [R_{i-1} d_i + p_{i-1} \times (R_{i-1} \delta_i)] \\ \delta_N^w &= \sum_{i=1}^{N} R_{i-1} \delta_i \end{aligned} \tag{A-24}$$

From Eq. (A-24), it is easy to see that the variation in the world coordinates system is not only related to the differential rotation δ_i and translation d_i in individual frame, but also dependent on rotational matrix (R_{i-1}) and transitional vector (p_{i-1}) relative to the base frame. The differential translational and rotational vectors in the individual frame are converted those in the world coordinate system by Eq. (A-24), where R_{i-1} is the 3×3 rotational matrix and p_{i-1} is the 3×1 positional vector of T_{i-1} defined by Eq. (A-2) above and the matrix T_{i-1} is a transformation between the $(i-1)$th and the base frames. However, in Mantripragada and Whitney's work [1,37], the positional vector and rotational matrix are taken to be p_i^- and R_i^- instead, respectively, which are defined by relative transition and rotation from the transformation A_{i-1} between the $(i-2)$th and the $(i-1)$th frames in Eq. (A-3), thus the differential translational and rotational vectors in the individual frame cannot be transformed into those in the world coordinate system. The further variation propagation control, which is based on this conversion, cannot handle the misorientation and misposition of the components.

Eq. (A-24) can be rewritten as:

$$\begin{aligned} d_N^w = \sum_{i=1}^{N} \Big\{ & [R_{i-1} m_{1i} \Delta X_i + R_{i-1} m_{2i} \Delta Y_i + R_{i-1} m_{3i} \Delta Z_i] \\ & + [R_{i-1} m_{4i} + p_{i-1} \times (R_{i-1} m_{7i})] \Delta x_i + [R_{i-1} m_{5i} + p_{i-1} \\ & \times (R_{i-1} m_{8i})] \Delta y_i + [R_{i-1} m_{6i} + p_{i-1} \times (R_{i-1} m_{9i})] \Delta z_i \Big\} \end{aligned} \tag{A-25}$$

$$\delta_N^w = \sum_{i=1}^{N} R_{i-1} m_{7i} \Delta x_i + \sum_{i=1}^{N} R_{i-1} m_{8i} \Delta y_i + \sum_{i=1}^{N} R_{i-1} m_{9i} \Delta z_i \tag{A-26}$$

Eqs. (A-25) and (A-26) can also be rewritten as follows:

$$d_N^w = W_1 \Delta X + W_2 \Delta Y + W_3 \Delta Z + W_4 \Delta x + W_6 \Delta y + W_8 \Delta z \tag{A-27}$$

$$\delta_N^w = W_5 \Delta x + W_7 \Delta y + W_9 \Delta z \tag{A-28}$$

where $\Delta X = \begin{bmatrix} \Delta X_1 & \cdots & \Delta X_N \end{bmatrix}^T$, $\Delta Y = \begin{bmatrix} \Delta Y_1 & \cdots & \Delta Y_N \end{bmatrix}^T$, $\Delta Z = \begin{bmatrix} \Delta Z_1 & \cdots & \Delta Z_N \end{bmatrix}^T$, $\Delta x = \begin{bmatrix} \Delta x_1 & \cdots & \Delta x_N \end{bmatrix}^T$, $\Delta y = \begin{bmatrix} \Delta y_1 & \cdots & \Delta y_N \end{bmatrix}^T$ and $\Delta z = \begin{bmatrix} \Delta z_1 & \cdots & \Delta z_N \end{bmatrix}^T$.

Combining Eqs. (A-27) and (A-28) gives:

$$\begin{aligned} \begin{bmatrix} d_N^w \\ \delta_N^w \end{bmatrix} = & \begin{bmatrix} W_1 \\ 0 \end{bmatrix} \Delta X + \begin{bmatrix} W_2 \\ 0 \end{bmatrix} \Delta Y + \begin{bmatrix} W_3 \\ 0 \end{bmatrix} \Delta Z + \begin{bmatrix} W_4 \\ W_5 \end{bmatrix} \Delta x \\ & + \begin{bmatrix} W_6 \\ W_7 \end{bmatrix} \Delta y + \begin{bmatrix} W_8 \\ W_9 \end{bmatrix} \Delta z \end{aligned} \tag{A-29}$$

Eqs. (A-29) can also be expressed as:

$$\begin{aligned} \begin{bmatrix} dx_N^w \\ dy_N^w \\ dz_N^w \\ \delta x_N^w \\ \delta y_N^w \\ \delta z_N^w \end{bmatrix} = & \begin{bmatrix} W_{(1,1),1} & W_{(1,1),2} & \cdots & W_{(1,1),i} & \cdots & W_{(1,1),N} \\ W_{(1,2),1} & W_{(1,2),2} & \cdots & W_{(1,2),i} & \cdots & W_{(1,2),N} \\ W_{(1,3),1} & W_{(1,3),2} & \cdots & W_{(1,3),i} & \cdots & W_{(1,3),N} \\ 0 & 0 & 0 & 0 & 0 & 0 \\ 0 & 0 & 0 & 0 & 0 & 0 \\ 0 & 0 & 0 & 0 & 0 & 0 \end{bmatrix} \begin{bmatrix} \Delta X_1 \\ \Delta X_2 \\ \vdots \\ \Delta X_i \\ \vdots \\ \Delta X_N \end{bmatrix} \\ & + \begin{bmatrix} W_{(2,1),1} & W_{(2,1),2} & \cdots & W_{(2,1),i} & \cdots & W_{(2,1),N} \\ W_{(2,2),1} & W_{(2,2),2} & \cdots & W_{(2,2),i} & \cdots & W_{(2,2),N} \\ W_{(2,3),1} & W_{(2,3),2} & \cdots & W_{(2,3),i} & \cdots & W_{(2,3),N} \\ 0 & 0 & 0 & 0 & 0 & 0 \\ 0 & 0 & 0 & 0 & 0 & 0 \\ 0 & 0 & 0 & 0 & 0 & 0 \end{bmatrix} \begin{bmatrix} \Delta Y_1 \\ \Delta Y_2 \\ \vdots \\ \Delta Y_i \\ \vdots \\ \Delta Y_N \end{bmatrix} \\ & + \begin{bmatrix} W_{(3,1),1} & W_{(3,1),2} & \cdots & W_{(3,1),i} & \cdots & W_{(3,1),N} \\ W_{(3,2),1} & W_{(3,2),2} & \cdots & W_{(3,2),i} & \cdots & W_{(3,2),N} \\ W_{(3,3),1} & W_{(3,3),2} & \cdots & W_{(3,3),i} & \cdots & W_{(3,3),N} \\ 0 & 0 & 0 & 0 & 0 & 0 \\ 0 & 0 & 0 & 0 & 0 & 0 \\ 0 & 0 & 0 & 0 & 0 & 0 \end{bmatrix} \begin{bmatrix} \Delta Z_1 \\ \Delta Z_2 \\ \vdots \\ \Delta Z_i \\ \vdots \\ \Delta Z_N \end{bmatrix} \\ & + \begin{bmatrix} W_{(4,1),1} & W_{(4,1),2} & \cdots & W_{(4,1),i} & \cdots & W_{(4,1),N} \\ W_{(4,2),1} & W_{(4,2),2} & \cdots & W_{(4,2),i} & \cdots & W_{(4,2),N} \\ W_{(4,3),1} & W_{(4,3),2} & \cdots & W_{(4,3),i} & \cdots & W_{(4,3),N} \\ W_{(5,1),1} & W_{(5,1),2} & \cdots & W_{(5,1),i} & \cdots & W_{(5,1),N} \\ W_{(5,2),1} & W_{(5,2),2} & \cdots & W_{(5,2),i} & \cdots & W_{(5,2),N} \\ W_{(5,3),1} & W_{(5,3),2} & \cdots & W_{(5,3),i} & \cdots & W_{(5,3),N} \end{bmatrix} \begin{bmatrix} \Delta\theta x_1 \\ \Delta\theta x_2 \\ \vdots \\ \Delta\theta x_i \\ \vdots \\ \Delta\theta x_N \end{bmatrix} \\ & + \begin{bmatrix} W_{(6,1),1} & W_{(6,1),2} & \cdots & W_{(6,1),i} & \cdots & W_{(6,1),N} \\ W_{(6,2),1} & W_{(6,2),2} & \cdots & W_{(6,2),i} & \cdots & W_{(6,2),N} \\ W_{(6,3),1} & W_{(6,3),2} & \cdots & W_{(6,3),i} & \cdots & W_{(6,3),N} \\ W_{(7,1),1} & W_{(7,1),2} & \cdots & W_{(7,1),i} & \cdots & W_{(7,1),N} \\ W_{(7,2),1} & W_{(7,2),2} & \cdots & W_{(7,2),i} & \cdots & W_{(7,2),N} \\ W_{(7,3),1} & W_{(7,3),2} & \cdots & W_{(7,3),i} & \cdots & W_{(7,3),N} \end{bmatrix} \begin{bmatrix} \Delta\theta y_1 \\ \Delta\theta y_2 \\ \vdots \\ \Delta\theta y_i \\ \vdots \\ \Delta\theta y_N \end{bmatrix} \\ & + \begin{bmatrix} W_{(8,1),1} & W_{(8,1),2} & \cdots & W_{(8,1),i} & \cdots & W_{(8,1),N} \\ W_{(8,2),1} & W_{(8,2),2} & \cdots & W_{(8,2),i} & \cdots & W_{(8,2),N} \\ W_{(8,3),1} & W_{(8,3),2} & \cdots & W_{(8,3),i} & \cdots & W_{(8,3),N} \\ W_{(9,1),1} & W_{(9,1),2} & \cdots & W_{(9,1),i} & \cdots & W_{(9,1),N} \\ W_{(9,2),1} & W_{(9,2),2} & \cdots & W_{(9,2),i} & \cdots & W_{(9,2),N} \\ W_{(9,3),1} & W_{(9,3),2} & \cdots & W_{(9,3),i} & \cdots & W_{(9,3),N} \end{bmatrix} \begin{bmatrix} \Delta\theta z_1 \\ \Delta\theta z_2 \\ \vdots \\ \Delta\theta z_i \\ \vdots \\ \Delta\theta z_N \end{bmatrix} \end{aligned} \tag{A-30}$$

where

$$W_{li}(3\times 1\,vector)=\begin{bmatrix}W_{(l,1),i}\\W_{(l,2),i}\\W_{(l,3),i}\end{bmatrix},\quad l=1,2,\ldots,9,$$

$W_{1i}=R_{i-1}m_{1i}$, $W_{2i}=R_{i-1}m_{2i}$, $W_{3i}=R_{i-1}m_{3i}$, $W_{4i}=R_{i-1}m_{4i}+p_{i-1}\times(R_{i-1}m_{7i})$, $W_{5i}=R_{i-1}m_{7i}$, $W_{6i}=R_{i-1}m_{5i}+p_{i-1}\times(R_{i-1}m_{8i})$, $W_{7i}=R_{i-1}m_{8i}$, $W_{8i}=R_{i-1}m_{6i}+p_{i-1}\times(R_{i-1}m_{9i})$ and $W_{9i}=R_{i-1}m_{9i}$.

Eq. (A-30) can be expressed as state transition model as follows:

$$\begin{bmatrix}dx_k^w\\dy_k^w\\dz_k^w\\\delta x_k^w\\\delta y_k^w\\\delta z_k^w\end{bmatrix}=\begin{bmatrix}dx_{k-1}^w\\dy_{k-1}^w\\dz_{k-1}^w\\\delta x_{k-1}^w\\\delta y_{k-1}^w\\\delta z_{k-1}^w\end{bmatrix}+\begin{bmatrix}W_{(1,1),k}&W_{(2,1),k}&W_{(3,1),k}&W_{(4,1),k}&W_{(6,1),k}&W_{(8,1),k}\\W_{(1,2),k}&W_{(2,2),k}&W_{(3,1),k}&W_{(4,2),k}&W_{(6,1),k}&W_{(8,2),k}\\W_{(1,3),k}&W_{(2,3),k}&W_{(3,1),k}&W_{(4,3),k}&W_{(6,1),k}&W_{(8,3),k}\\0&0&0&W_{(5,1),k}&W_{(7,1),k}&W_{(9,1),k}\\0&0&0&W_{(5,2),k}&W_{(7,2),k}&W_{(9,2),k}\\0&0&0&W_{(5,3),k}&W_{(7,3),k}&W_{(9,3),k}\end{bmatrix}\times\begin{bmatrix}\Delta X_k\\\Delta Y_k\\\Delta Z_k\\\Delta\theta x_k\\\Delta\theta y_k\\\Delta\theta z_k\end{bmatrix}\tag{A-31}$$

Eq. (A-31) relates the total differential rotation vector and differential translation vector.

A.3. Cartesian position and orientation errors in the world coordinate

The correct position is:

$$T_N^c=T_N+dT_N=(I+\delta T_N^w)T_N\tag{A-32}$$

To separate the rotational components and translational components of the correct position, as described in [35], T_N can be written in the following form

$$T_N=\begin{bmatrix}R_N&p_N\\0&1\end{bmatrix}\tag{A-33}$$

and δT_N^w can be written as

$$\delta T_N^w=\begin{bmatrix}\delta R_N^w&d_N^w\\0&0\end{bmatrix}\tag{A-34}$$

From Eqs. (A-32)–(A-34), the resulting rotational components and translational components can be written as

$$R_N^c=(I+\delta R_N^w)R_N\tag{A-35}$$

and

$$p_N^c=p_N+(\delta_N^w\times p_N)+d_N^w\tag{A-36}$$

If the correct Cartesian position is expressed as

$$p_N^c=p_N+dp\tag{A-37}$$

Then from Eqs. (A-36) and (A-37) the first-order differential error in the Cartesian position of the end-effector as follows:

$$dp=(\delta_N^w\times p_N)+d_N^w\tag{A-38}$$

Thus the error of final matrix transform in the world coordinate system is:

$$\delta T=\begin{bmatrix}0&-\delta z_N^w&\delta y_N^w&dp_N^X\\\delta z_N^w&0&-\delta x_N^w&dp_N^Y\\-\delta y_N^w&\delta x_N^w&0&dp_N^Z\\0&0&0&0\end{bmatrix}\tag{A-39}$$

and final matrix transform can be obtained by Eqs. (A-30), (A-38) and (A-39).

Thus Cartesian position error in the world coordinate system at Stage k is:

$$dp_k=\begin{bmatrix}dp_k^X\\dp_k^Y\\dp_k^Z\end{bmatrix}=\delta_k^w\times p_k+d_k^w\tag{A-40}$$

Cartesian orientation error in the world coordinate system at Stage k is:

$$\delta_k^w=\begin{bmatrix}\delta x_k^w\\\delta y_k^w\\\delta z_k^w\end{bmatrix}\tag{A-41}$$

References

[1] Mantripragada R, Whitney DE. Modeling and controlling variation propagation in mechanical assemblies using state transition models. IEEE Transactions on Robotics and Automation 1999;15:124–40.
[2] Carnelio JA, Yim H. Identification of dimensional variation patterns on compliant assemblies. Journal of Manufacturing Systems 2006;25:65–76.
[3] Huang W, Kong Z. Simulation and integration of geometric and rigid body kinematics errors for assembly variation analysis. Journal of Manufacturing Systems 2008;27:36–44.
[4] Camelio JA, Jack Hu S, Ceglarek D. Impact of fixture design on sheet metal assembly variation. Journal of Manufacturing Systems 2004;23:182–93.
[5] Cai W. A new tolerance modeling and analysis methodology through a two-step linearization with applications in automotive body assembly. Journal of Manufacturing Systems 2008;27:26–35.
[6] Lin CY, Huang WH, Jeng MC, Doong JL. Study of an assembly tolerance allocation model based on Monte Carlo simulation. Journal of Materials Processing Technology 1997;70:9–16.
[7] Thimm G, Britton G, Cheong FS. Controlling tolerance stacks for efficient manufacturing. The International Journal of Advanced Manufacturing Technology 2001;18:44–8.
[8] Forouraghi B. Worst-case tolerance design and quality assurance via genetic algorithms. Journal of Optimization Theory and Applications 2002;13:251–68.
[9] Dantan JY, Qureshi AJ. Worst-case and statistical tolerance analysis based on quantified constraint satisfaction problems and Monte Carlo simulation. Computer-Aided Design 2009;41:1–12.
[10] Spolts MF. Design of machine elements. Englewood Cliffs, New Jersey: Prentice-Hall; 1971.
[11] Arron DD, Walter JM, Charles EW. Machine design theory and practices. New York: MacMillan; 1975.
[12] He JR. Estimating the distributions of manufactured dimensions with the beta probability density function. International Journal of Machine Tools and Manufacture 1991;31:383–96.
[13] Nigam SD, Turner JU. Review of statistical approaches to tolerance analysis. Computer-Aided Design 1995;27:6–15.
[14] Mease D, Nair VN, Sudjianto A. Selective assembly in manufacturing. Technometrics 2004;46:165–75.
[15] Rachuri S, Han YH, Foufou S, Feng SC, Roy U, Wang F, et al. A model for capturing product assembly information. Journal of Computing and Information Science in Engineering 2006;3:11–21.
[16] Jin J, Shi J. State space modeling of sheet metal assembly for dimensional control. Journal of Manufacturing Science and Engineering 1999;121:756–62.

[17] Shi J. Stream of variation modeling and analysis for multistage manufacturing processes. CRC Press, Taylor & Francis Group; 2006.
[18] Shi J, Zhou S. Quality control and improvement for multistage systems: a survey. IIE Transactions on Quality and Reliability Engineering 2009;41:744–53.
[19] Liu J, Jin J, Shi J. State space modeling for 3-dimensional variation propagation in rigid-body multistage assembly processes. IEEE Transactions on Automation Science and Engineering 2010;7:274–90.
[20] Ding Y, Ceglarek D, Shi J. Modeling and diagnosis of multistage manufacturing process. Part I. State space model. In: Japan/USA symposium on flexible automation. 2000.
[21] Ragu K, Mohanram PV. Tolerance design of multistage radial flow submersible pumps. Mechanika 2007;63:64–70.
[22] Gunston B. Rolls-Royce aero engines. England: Patrick Stephens Limited; 1989.
[23] Klocke F, Veselovac D, Auerbach T, Seidner R. Intelligent assembly for aero engine components. In: Intelligent robotics and applications. Berlin/Heidelberg: Springer; 2008.
[24] Mears ML. Geometry estimation and adaptive actuation for centering preprocessing and precision measurement. Dissertation, Mechanical Engineering, Georgia Institute of Technology; 2006.
[25] Roy U, Li B. Representation and interpretation of geometric tolerances for polyhedral objects. I. Form tolerances. Computer-Aided Design 1998;30:151–61.
[26] Roy U, Li B. Representation and interpretation of geometric tolerances for polyhedral objects. II. Size, orientation and position tolerances. Computer-Aided Design 1999;31:273–85.
[27] Cai M, Yang JX, Wu ZT. Mathematical model of cylindrical form tolerance. Journal of Zhejing University Science 2004;5:890–5.
[28] Whitney DE. Mechanical assemblies. Oxford: Oxford University Press; 2004.
[29] Chen KZ, Feng XA, Lu QS. Intelligent location-dimensioning of cylindrical surfaces in mechanical parts. Computer-Aided Design 2002;34:185–94.
[30] Whitney DE, Gilbert OL. Representation of geometric variations using matrix transforms for statistical tolerance analysis in assemblies. In: Proceedings of the IEEE international conference on robotics and automation. 1993.
[31] Whitney DE, Gilbert OL, Jastrzebski M. Representation of geometric variations using matrix transforms for statistical tolerance analysis in assemblies. Research in Engineering Design 1996;6:191–210.
[32] Paul RP. Robot manipulators: mathematics, programming, and control. Cambridge: The MIT Press; 1981.
[33] Pieper DL. The kinematics of manipulators under computer control. Stanford Artificial Intelligence Laboratory, Stanford University, AIM 72; 1968.
[34] Denavit J, Hartenberg RS. A kinematic notation for lower-pair mechanisms based on matrices. Journal of Applied Mechanics 1955;6:215–21.
[35] Veitschegger WK, Wu CH. Robot accuracy analysis based on kinematics. IEEE Journal of Robotics and Automation 1986;2:171–9.
[36] Wu CH. A CAD tool for the kinematic design of robot manipulator. In: International conference on advanced automation. 1983.
[37] Mantripragada R. Assembly oriented design: concepts, algorithms and computational tools. Ph.D. thesis, Mechanical Engineering, Massachusetts Institute of Technology; 1998.